ESLAB #53: The *Gaia* Universe
Unedited (Zenodo community curated by J.H.J. de Bruijne)

Relics of the Formation of the Galactic Halo from Gaia and APOGEE

Paola Re Fiorentin[1], Mario G. Lattanzi[1], Alessandro Spagna[1]

[1] INAF - Osservatorio Astrofisico di Torino, Strada Osservatorio 20, 10025 Pino Torinese, TO, Italy

Abstract

The solar neighborhood potentially contains a very large number of kinematic groups which are related to the various building blocks of the stellar halo. We explore the vicinity of the Milky Way through the use of high quality astrometric and spectroscopic data from the most recent releases by Gaia and APOGEE. We chemically select 663 halo stars and analyse their kinematics and orbital properties in order to investigate and characterise the possibly detectable signatures that remain in phase-space. We find evidence of statistically significant substructures among 177 stars, with velocity difference less than 20 km s^{-1}, that are classified in $15-25$ kinematic groups and compared to the high velocity streamers by Re Fiorentin et al. 2015. The signal is even stronger among the stars with $[\mathrm{Mg/Fe}] \leq 0.2$ dex, that more likely have been accreted; preliminary results are shown. The chemical properties of the kinematically selected moving groups are going to be analysed to reconstruct the accretion history of the stellar halo.

1 Introduction

According to the hierarchical structure formation model, galaxies like the Milky Way grow by mergers of dwarf galaxies; this theory predicts, especially in the stellar halos, the presence of fossil substructures due to accretions experienced over their lifetime.

Simulations based on this cosmological paradigm have shown that low mass stellar systems orbiting a host galaxy undergo disruption and distortion due to the action of tidal forces. This process rips out stars from the progenitor and leads to the formation of merger debris with an inhomogeneous distribution of stars of the spheroidal halolike component (Johnston 1998; Harding et al. 2001; Bullock & Johnston 2005; Cooper et al. 2010; Helmi et al. 2011; Gomez et al. 2013; Starkenburg et al. 2009, 2013; Murante et al. 2010, 2015).

Detailed studies of the halo of our own Galaxy are important for understanding the formation and evolution of the Milky Way in a cosmological context (Searle & Zinn 1978; Freeman & Bland-Hawthorn 2002).

Considerable structure is still present in the Galactic halo that do retain memory of its accretion history in the form of streams of stars (e.g. Helmi 2008; Malhan et al. 2018). In the solar neighborhood, where strong phase-mixing takes place, merger debris may be detectable as stellar groups with coherent kinematics despite being of very low spatial density (Helmi et al. 1999; Smith et al. 2009; Klement 2010; Re Fiorentin et al. 2015; Belokurov et al. 2018; Helmi et al. 2018). However, the number of such substructures due to accreted stars is still smaller than expected.

Large samples of stars with accurate 6D phase-space information and complete chemical properties for classification and following characterisation are needed. This information can be obtained from massive astrometric and spectrophotometric surveys; indeed, with the high-precision data already, or soon to be available, a golden age for Galactic studies has started.

The Gaia second data release (DR2; Gaia Collaboration 2018) provides unprecedented accurate measurements of parallax and proper motion for more than 1.3 billion stars across the whole sky (Lindegren et al. 2018). The Apache Point Observatory Galactic Evolution Experiment fourteenth data release, APOGEE DR14, has delivered high-resolution ($R \sim 22\,500$) high signal-to-noise near-infrared spectra, enabling the determination of precise radial velocities as well as stellar parameters and abundances for more than 20 chemical elements (Majewski et al. 2017; Abolfathi et al. 2018).

Here, we show the excellent synergy between Gaia and APOGEE, and take advantage of high-quality data in order to study chemo-kinematic signatures in the local halo.

Section 2 describes our selection of halo stars, Section 3 presents findings that resulted from our analysis, while Section 4 recaps conclusions and addresses future works.

2 Data

This study is based on a new kinematic catalogue, assembled after cross-matching Gaia DR2 and APOGEE DR14.

For 170 303 common objects, it contains DR2 positions, parallaxes and proper motions (Lindegren et al. 2018), plus radial velocities and chemical abundances derived with the APOGEE Stellar Spectra Parameter Pipeline (e. g., Holtzman et al. 2015; Garcia et al. 2016). This data set is used to derive and exploit a complete six-dimensional phase-space information for a sufficiently *pure* chemically selected tracers of the halo population.

We use Gaia DR2 sources for which a five-parameters astrometric solution (sky positions, parallax and proper motions; *astrometric_params_solved* = 31) is available with its corresponding covariances and remove astrometric binaries and anomalous cases (i. e., *astrometric_excess_noise=0* or *astrometric_excess_noise_sig* < 2). Then, we retain only those stars with relative parallax error $\varpi/\sigma_\varpi > 5$, that allows to compute distances as $d = 1/\varpi$. In addition, in order to work with reliable α-element abundances, we reject stars with flags warning of poor stellar parameter estimates and we only consider stars with signal-to-noise ratios greater than 70, $\chi^2 < 10$ and $4000 < T_{\rm eff} < 5000$ K (see also

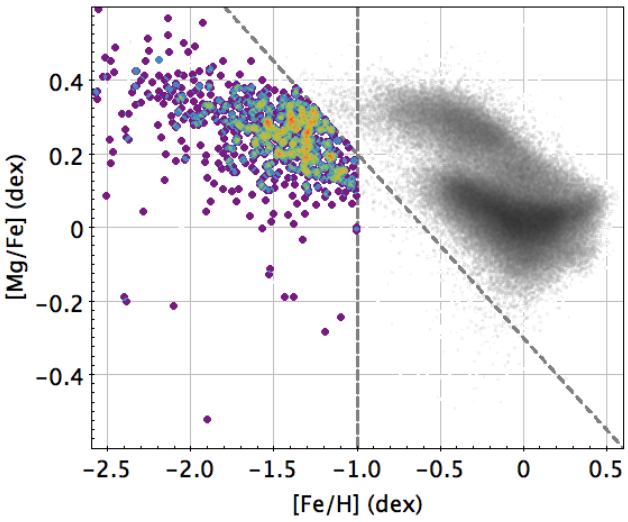

Figure 1: Chemical distribution, [Mg/Fe] vs. [Fe/H], for the 67 358 Gaia DR2-APOGEE DR14 stars. The dashed lines represent the adopted separation between halo stars having [Fe/H] < 1 dex (below) and thick/thin disk stars (above). Typical errors are below 0.03 dex per [α/Fe] and less than 0.07 dex per [Fe/H].

Re Fiorentin et al. 2019 and references therein).

After the above astrometric and spectroscopic selections, our initial sample comprises a total of 69 400 red giants down to $G = 17.73$ mag with only 26 stars fainter than 16.5 mag. Median uncertainties are: 0.03 mas in parallax, 50 μas yr^{-1} in proper motion, and ~ 100 m s^{-1} for the APOGEE line-of-sight velocities.

Galactic space-velocity components[1] are derived by assuming that the Sun is 8.5 kpc away from the Milky Way centre, the LSR rotates at 232 km s^{-1} around the Galactic centre (McMillan 2017), and the LSR peculiar velocity of the Sun is $(U, V, W)_\odot = (11.1, 12.24, 7.25)$ km s^{-1} (Schoenrich et al. 2010). Median uncertainties of the Galactocentric velocities are below 0.6 km s^{-1} per component.

Figure 1 shows the chemical plane, [α/Fe] vs. [Fe/H], for the full kinematic catalog. Clearly, the sample includes thin and thick disk stars. Halo stars with [Fe/H] < -1 dex are chemically identified, according to Mackereth et al. 2019, by the relation:

$$[\mathrm{Mg/Fe}] < -0.2 - 0.5 \cdot ([\mathrm{Fe/H}] + 0.2). \quad (1)$$

In the following kinematic analysis we exclude spectroscopic binaries and members of globular clusters (e.g. M13). With this further selection our sample is composed of 663 halo stars.

The spatial distribution of the selected halo sample is shown in Fig. 2. Stars with [Mg/Fe] ≤ 0.2 dex are marked as red dots; these 195 low-α objects are more likely accreted stars (e.g. Di Matteo et al. 2018).

[1]We adopt the convention of U, V, and W oriented towards the Galactic centre, the direction of Galactic rotation, and the north Galactic pole, respectively.

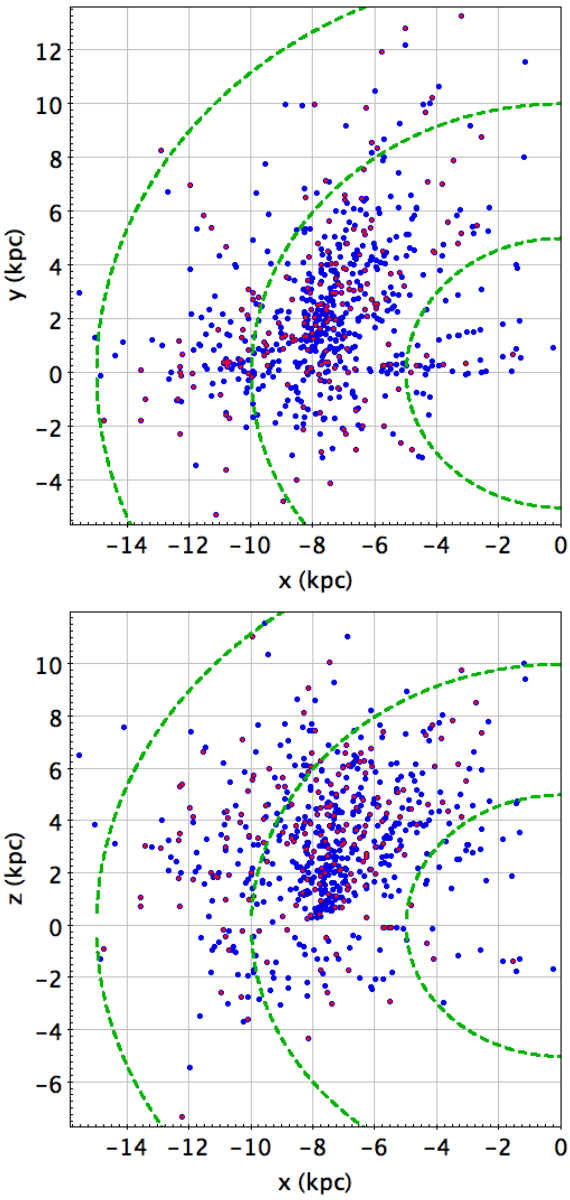

Figure 2: Spatial distribution of the 663 chemically selected nearby halo stars in the $x-y$ (top) and $x-z$ (bottom) plane. Stars with [Mg/Fe] ≤ 0.2 dex (195) are marked as red dots. Dashed lines show the locus of objects at a distance from the Galactic centre, $(0; 0; 0)$, $R = 5, 10, 15$ kpc. The Sun is located at $(-8; 0; 0)$ kpc.

3 Results

The velocity distribution of the chemically selected sample is given in Fig. 3. It is consistent with an halo population; clearly clumps and overdensities of moving groups are present among the full sample (blue) as well as the subset of low-α stars (red).

3.1 Kinematic analysis

In order to quantify the deviations from a smooth distribution and the presence of kinematic substructures, we com-

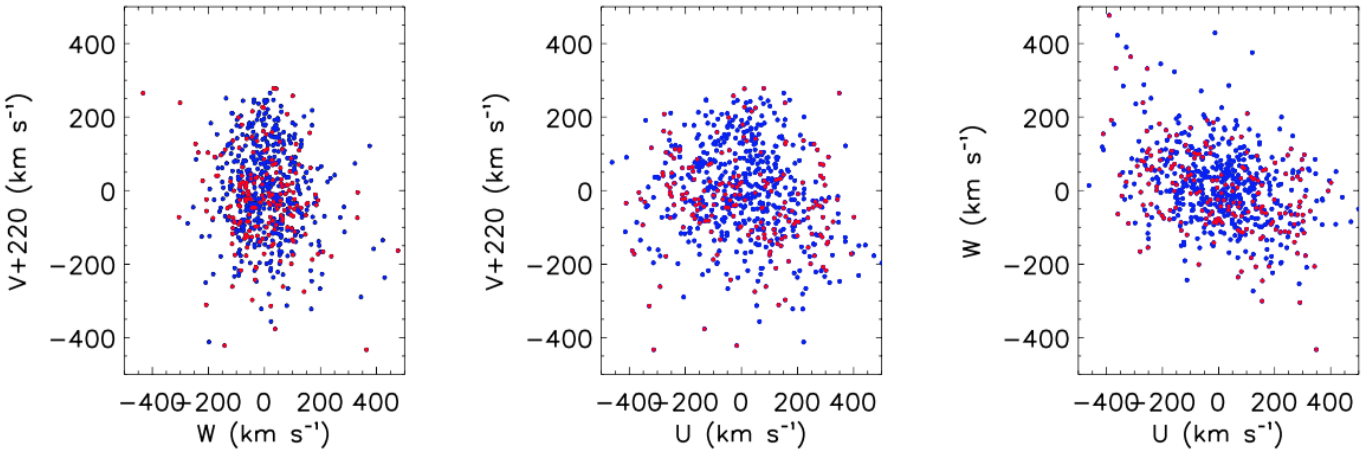

Figure 3: Velocity distribution of the chemically selected halo sample shown in Fig. 2.

pute, on the paired velocity differences, the cumulative two-point velocity correlation function as:

$$\xi(|\mathbf{v_i} - \mathbf{v_j}|) = \frac{\langle DD \rangle}{\langle RR \rangle} - 1. \quad (2)$$

where, $\langle DD \rangle$, the number of pairs of stars in our data within a given velocity difference, is compared to the one, $\langle RR \rangle$, from a representative random smooth sample[2].

In practice, a statistical excess of stars with small pairwise velocity differences indicates the presence of possible streamers made of objects with coherent kinematics.

Figure 4 shows, using bins of 10 $\mathrm{km\,s^{-1}}$ width, the two-point correlation function ξ for the full sample of 663 halo stars (filled dots), and separately for the subsample of 195 stars with $[\mathrm{Mg/Fe}] \leq 0.2$ dex (diamonds). There is a statistically significant signal ($SNR > 4$) for the full sample, that peaks at 20 $\mathrm{km\,s^{-1}}$; it appears even stronger for the low-α subset.

3.2 Clustering and Orbital Properties

In the following, we report a preliminary analysis of the full sample. We focus on the objects with paired velocity differences less than 20 $\mathrm{km\,s^{-1}}$, which yield the statistically significant signal seen in Fig. 4. To make the analysis more robust we exclude groups with only two objects. The final sample is made of 177 stars.

In order to classify these objects into meaningful groups, we perform K-medoids clustering[3] in 3D velocity space. Here, we just recall that this unsupervised learning algorithm chooses data points as centers (medoids), and groups the remaining data into a pre-specified number K of clusters that minimizes the RMS of the distance (in velocity space) to the center of each cluster (for more details and discussions on the choice of the assumed known a priori number of clusters, refer to Re Fiorentin et al. 2015 and Hastie et al. 2001).

We adopted $K = 25$ as optimal solution. Among the velocity distribution of the full sample, the 15 most numerous

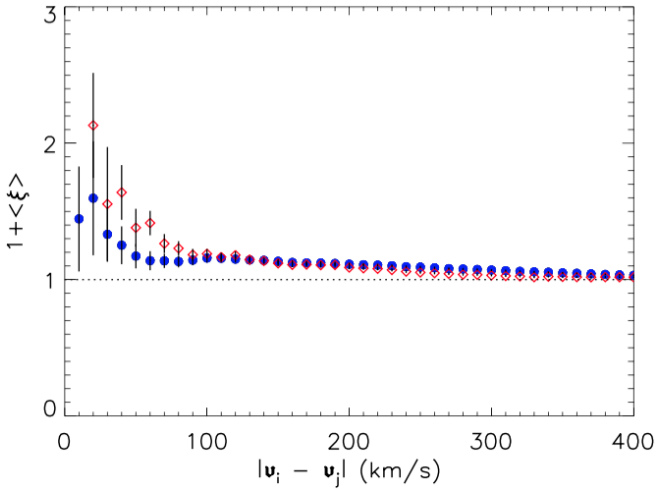

Figure 4: Cumulative velocity correlation function for the full sample of halo stars (filled dots), and the low-α subset (diamonds) shown in Fig. 3. The error bars are derived from Poisson's statistics of the counts.

kinematic substructures detected are visualized with different colors in Fig. 5.

For better identification of the different possible merging events that might have given rise to the observed substructures, we explore the "integrals of motion" space where the initial clumping of satellites are present even after the system has completely phase-mixed (e.g., Helmi & de Zeeuw 2000).

In this study, we look at the plane defined by the components of angular momentum in and out the plane of the Galaxy's disk, i.e., L_{xy} and L_z, respectively. Figure 5 visualizes the distribution of the chemically selected halo sample; highlighted in colors are the 15 kinematic moving groups with coherent kinematics identified (pairwise velocity differences less than 20 $\mathrm{km\,s^{-1}}$). Clearly, these cold streamers do appear clustered in this space. For comparison, we include Figure 4 by Re Fiorentin et al. 2015 who found high velocity streamers on retrograde and on high-inclination only prograde orbits.

[2]The actual random pairs are obtained after averaging independent realisations obtained from the observed data set by reshuffling the velocity components V and W, after fixing U.

[3]We used the implementation of the K-medoids clustering developed as part of the *R Project for Statistical Computing*: www.r-project.org.

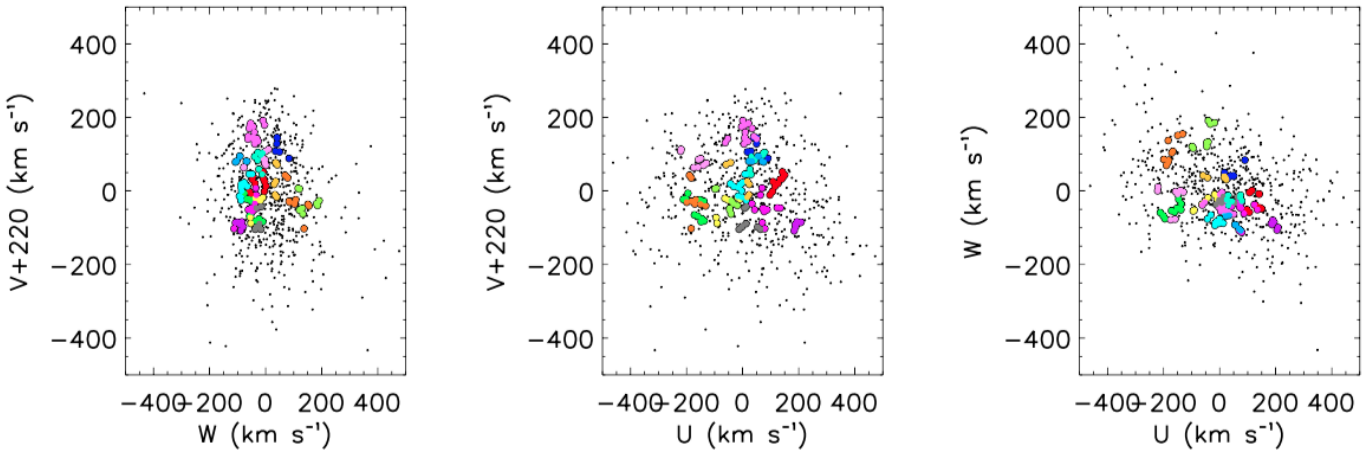

Figure 5: As Fig. 3. Among the full sample, circles identify objects with pairwise velocity difference less than 20 km s^{-1}. Different colors are used to indicate stars associated with the most numerous 15 clumps of the 25 recovered by the clustering analysis.

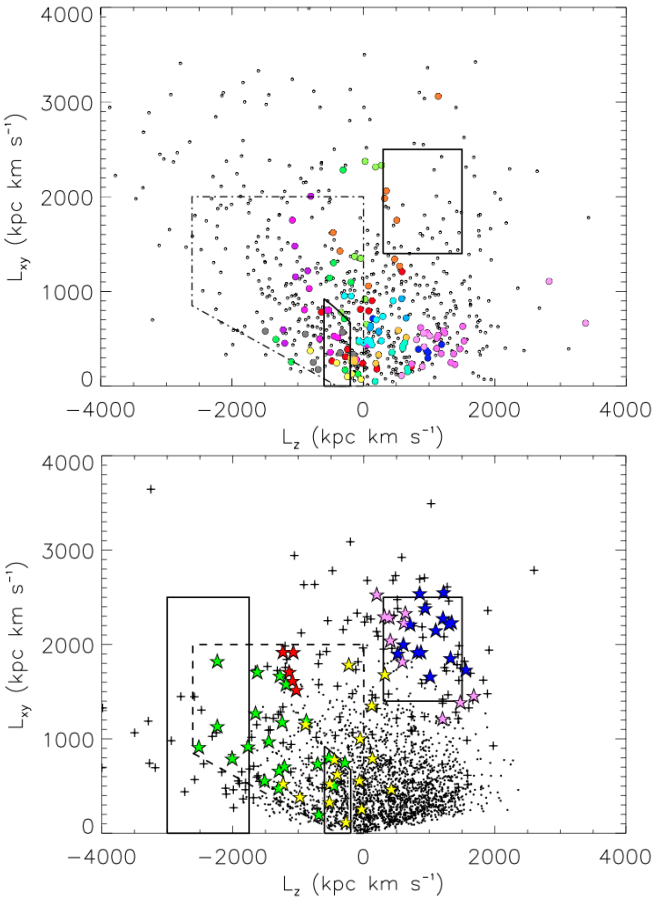

Figure 6: Space of adiabatic invariants $L_z - L_{xy}$. **Top:** As in Fig. 5, different colors are used to indicate the 15 clumps recovered by the clustering analysis in velocity space. Solid boxes show the locus of ω-Cen (at $L_z < 0$) and the Helmi stream (at $L_z > 0$); dashed box defines the region of the retrograde high velocity streamers by Re Fiorentin et al. 2015. **Bottom:** Their Figure 4, for direct comparison.

Now, low velocity streamers torn from their progenitors that appear to be also low-inclination prograde satellites have been detected.

4 Discussion and conclusions

From the cross-match between the Gaia DR2 and APOGEE DR14 catalogues, we have chemically selected samples of halo giants in the Solar neighborhood ($R < 15$ kpc) and carried out a first statistical analysis of their kinematics.

Based on clustering in velocity space, we found evidence of substructures in their motions. The signal is stronger for the subsample of stars with $[\mathrm{Mg/Fe}] \leq 0.2$ dex that we believe are tracers of the accreted halo sample. This is in line with previous studies and expected in a hierarchical universe.

Among the full sample, we found $15 - 25$ kinematic overdensities including several new groups in the low metallicity regime that we are going to further investigate by means of more detailed chemical analysis. Analysis of the group members with $[\mathrm{Mg/Fe}] \leq 0.2$ dex is in progress.

This methodology is certainly able to detect new streamers. Thus, it can be useful to address the problem of the missing debris in the inner halo, disentangle the matter on an accreted versus in situ halo, and to reconstruct the accretion history of the stellar halo.

Acknowledgments

This work has made use of data from the European Space Agency (ESA) mission Gaia (https://www.cosmos.esa.int/gaia), processed by the Gaia Data Processing and Analysis Consortium (DPAC, https://www.cosmos.esa.int/web/gaia/dpac/consortium). Funding for the DPAC has been provided by national institutions, in particular the institutions participating in the Gaia Multilateral Agreement. This work has been funded in part by the Italian Space Agency (ASI) under contract n. 2018-24-HH.0 "Gaia Mission - The Italian Participation in DPAC. Operations and Activities on Data Analysis". Funding for the Sloan Digital Sky Survey IV has been provided by the Alfred P. Sloan Foundation, the U.S. Department of Energy Office of Science, and the

Participating Institutions. SDSS acknowledges support and resources from the Center for High-Performance Computing at the University of Utah. The SDSS web site is www.sdss.org. SDSS is managed by the Astrophysical Research Consortium for the Participating Institutions of the SDSS Collaboration including the Brazilian Participation Group, the Canergie Institution for Science, Canergie Mellon University, the Chilean Participation Group, the French Participation Group, Harvard-Smithsonian Center for Astrophysics, Instituto de Astrofísica de Canarias, The Johns Hopkins University, Kavli Insitute for the Physics and Mathematics of the Universe (IPMU) / University of Tokyo, the Korean Participation Group, Lawrence Berkeley National Laboratory, Leibniz Institut für Astrophysik Potsdam (AIP), Max-Plank-Institut für Astronomie (MPIA Heidelberg), Max-Plank-Institut für Astrophysik (MPA Garching), Max-Plank-Institut für Extraterrestrische Physik (MPE), National Astronomical Observatories of China, New Mexico State University, New York University, University of Notre Dame, Observatório Nacional / MCTI, The Ohio State University, Pennsylvania State University, Shanghai Astronomical Observatory, United Kingdom Participation Group, Universidad Nacional Autonóma de México, University of Arizona, University of Colorado Boulder, University of Oxford, University of Portsmouth, University of Utah, University of Virginia, University of Washington, University of Wisconsin, Vanderbilt University, and Yale University.

References

Abolfathi, B., et al. 2018, ApJS, 235, 42
Belokurov, V., et al. 2018, MNRAS, 478, 611
Bullock, J. S., & Johnston, K. V. 2005, ApJ, 635, 931
Cooper, A. P., et al. 2010, MNRAS, 406, 744
Di Matteo, P., et al. 2018, arXiv:1812.08232
Freeman, K., & Bland-Hawthorn, J. 2002, ARA&A, 40, 487
Gaia Collaboration 2018, A&A, 616, A1
Garcia Perez A. E., et al. 2016, AJ, 151, 144
Gomez, F. A., et al. 2013, MNRAS, 436, 3602
Harding, P., et al. 2001, AJ, 122, 1397
Hastie, T., Tibshirani, R., & Friedman, J. 2001, The Elements of Statistical Learning (Berlin: Springer)
Helmi, A., et al. 1999, Nature, 402, 53
Helmi, A., & de Zeeuw, P. T. 2000, MNRAS, 319, 657
Helmi, A. 2008, A&AR, 15, 145
Helmi, A., et al. 2011, ApJL, 733, L7
Helmi, A., et al. 2018, Nature, 563, 85
Holtzman J. A., et al. 2015, AJ, 150, 148
Johnston, K. V. 1998, ApJ, 495, 297
Klement, R. J. 2010, A&AR, 18, 567
Lindegren L., et al. 2018, A&A, 616, A2
Mackereth, J. T., et al. 2019, MNRAS, 482, 3426
Majewski S. R., et al. 2017, AJ, 154, 94
McMillan P. J. 2017, MNRAS, 465, 76
Malhan, K., et al. 2018, MNRAS, 481, 3442
Murante, G., et al. 2010, ApJL, 716, L115
Murante, G., et al. 2015, MNRAS, 447, 178
Re Fiorentin, P., et al. 2015, AJ, 150, 128
Re Fiorentin, P., et al. 2019, MNRAS, 484, L69
Searle, L., & Zinn, R. 1978, ApJ, 225, 357
Schoenrich R., et al. 2010, MNRAS, 403, 1829
Smith, M. C., et al. 2009, MNRAS, 399, 1223
Starkenburg, E., et al. 2009, ApJ, 698, 567
Starkenburg, E., et al. 2013 MNRAS, 429, 725